

LA-UR-17-29718

Approved for public release; distribution is unlimited.

Title: 29 mm Diameter Target Test Report

Author(s): Woloshun, Keith Albert
Olivas, Eric Richard
Dale, Gregory E.
Naranjo, Angela Carol
Romero, Frank Patrick
Chemerisov, Sergey
Gromov, Roman

Intended for: Report

Issued: 2017-10-23

Disclaimer:

Los Alamos National Laboratory, an affirmative action/equal opportunity employer, is operated by the Los Alamos National Security, LLC for the National Nuclear Security Administration of the U.S. Department of Energy under contract DE-AC52-06NA25396. By approving this article, the publisher recognizes that the U.S. Government retains nonexclusive, royalty-free license to publish or reproduce the published form of this contribution, or to allow others to do so, for U.S. Government purposes. Los Alamos National Laboratory requests that the publisher identify this article as work performed under the auspices of the U.S. Department of Energy. Los Alamos National Laboratory strongly supports academic freedom and a researcher's right to publish; as an institution, however, the Laboratory does not endorse the viewpoint of a publication or guarantee its technical correctness.

29 mm Diameter Target Test Report

Keith Woloshun, Greg Dale, Eric Olivas, Alex Wass, Angela Naranjo, Frank Romero; LANL

Sergey Chemerisov, Roman Gromov; ANL

Rev. 1

10/17/2017

Introduction

After numerous delays, the test of the 29 mm diameter target was conducted on 8/18/2017. The complete target design report, dated 8/15/2016, is reproduced below for completeness. This describes in detail the 10 disk target with varying thickness disks. The report presents and discusses the test results. In brief summary, there appears to have been multiple instrumentation errors. Measured temperatures, pressures and IR camera window temperature measurement are all suspect. All tests were done at 35 MeV, with 171 μ A current, or 6 kW of beam power.

Data and Analysis

Data was collected at 2 pressures. As measured at PT-100, located on the pressure vessel, these pressures were 198 and 235 psig. However, with the blower off, at the 235 psig reading on PT-100, the pressure gage at the bottle location indicated 285 psig (1.965 MPa), cracking the pressure relief valve, which historically cracked open at this pressure. It was therefore assumed that the transducers in the beam area were defective. PT-101, located at the pump discharge was indicating 297 psig with the blower off. Given this uncertainty, data only at the higher pressure has been analyzed, and that pressure is assumed to be the 285 psi gage pressure as indicated outside the radiation area.

Target pressure drop as a function of flow rate, as measured at DP-101, was compared with that predicted by finite element analysis. This result is shown in Figure 1. The measured pressure drop was much higher than expected at all flow rates, although the transducer saturated at 20 psi. Further, subtracting the readings from the 2 absolute pressure transducers before and after the target indicates even higher pressure drop, 39 psi, far exceeding the capacity of the blower.

Temperature was intended to be measured on each of the first 6 disks. Unfortunately, signal was lost on the first 2 disks at the onset of the experiments, reading nominally room temperature throughout. The temperature of disks 3 through 6 consistently read very high compared to prediction. Calculated temperatures were made using finite element model and the Dittus-Bolter correlation: $Nu = 0.023 Re^{0.8}Pr^{0.333}$, with Nu the dimensionless heat transfer coefficient, Re the Reynolds number of the gas, and Pr the helium Prandtl number. Figures 2a,

2b and 2c show the comparison of the calculated and measured temperatures at 2 different Reynolds numbers (flow rates) at 285 psig. Ignoring the first 2 disks, the large discrepancy between measured and predicted is apparent. Either the measured temperatures are all inaccurate or the measured flow rate is too high. Figure 3 shows Nu vs Re for the data and 3 correlations for flow in channels. Clearly, the heat transfer measured is far below the predictions.

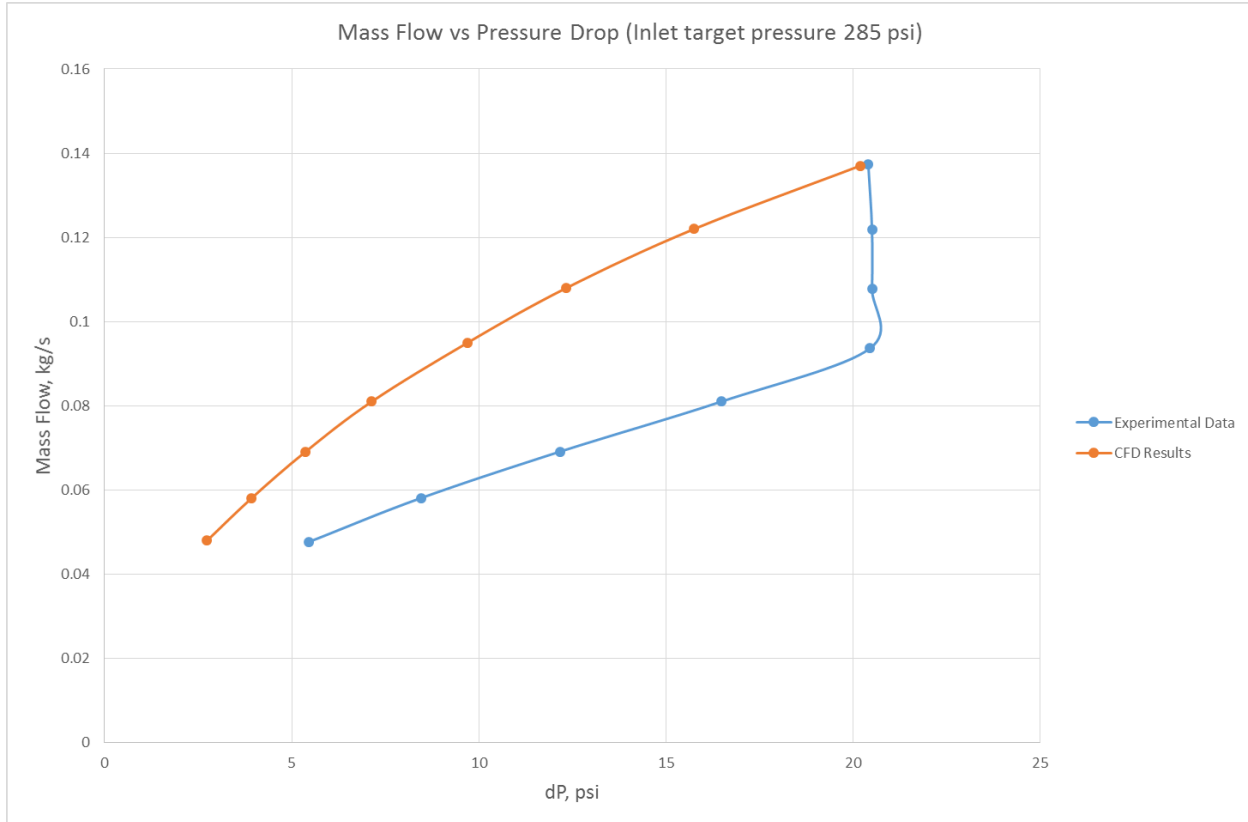


Figure 1. Target mass flow rate vs. pressure drop comparison of finite element model prediction and test data.

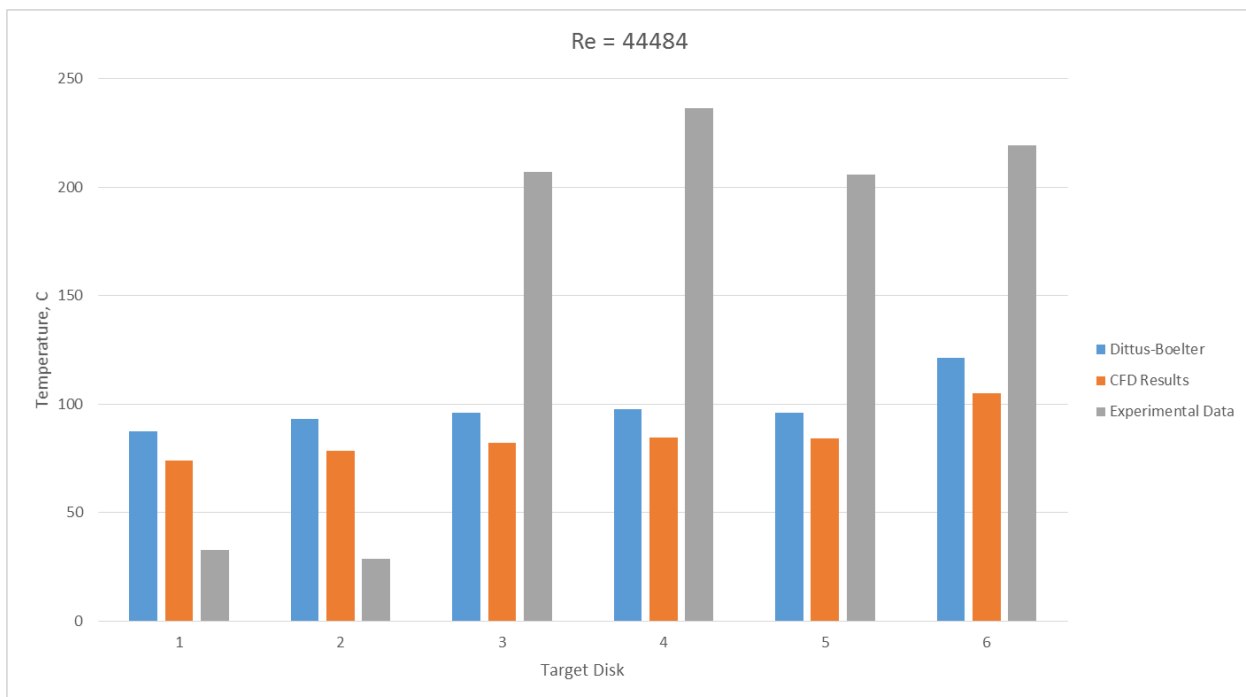


Figure 2a. Calculated and measured disk temperatures at Re= 44484 (137 g/s helium flow rate).

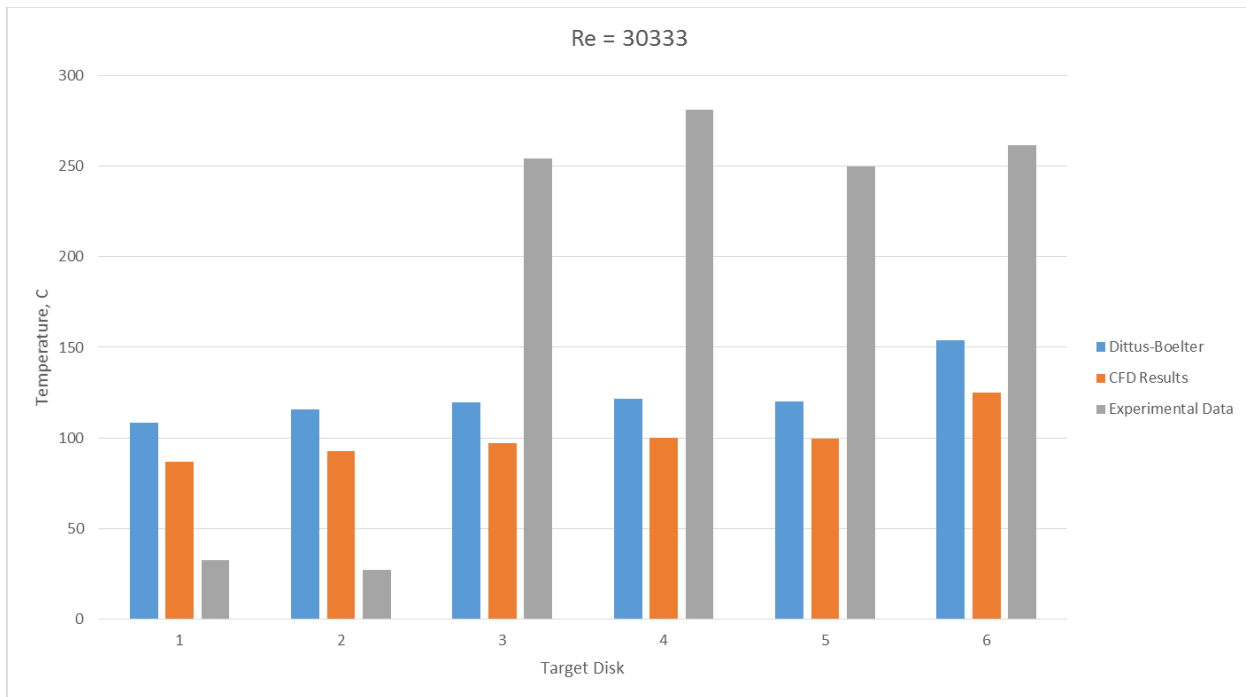


Figure 2b. Calculated and measured disk temperatures at Re= 30333 (93 g/s helium flow rate).

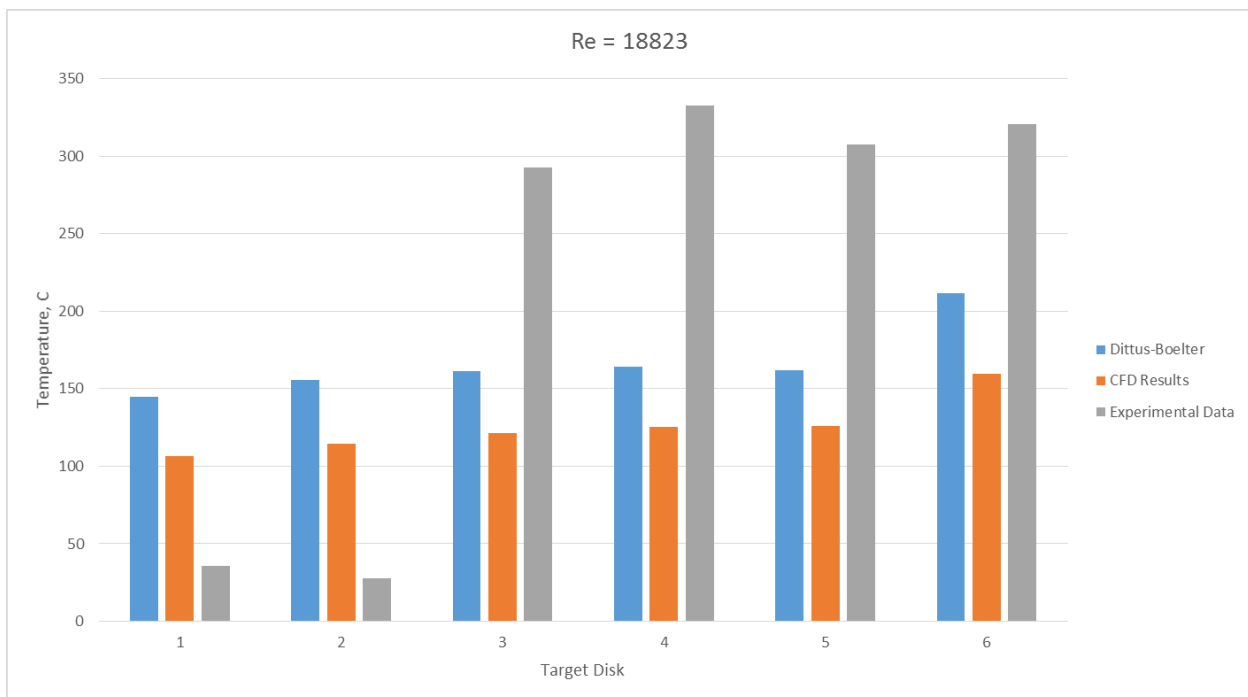


Figure 2c. Calculated and measured disk temperatures at $Re = 18823$ (58 g/s helium flow rate).

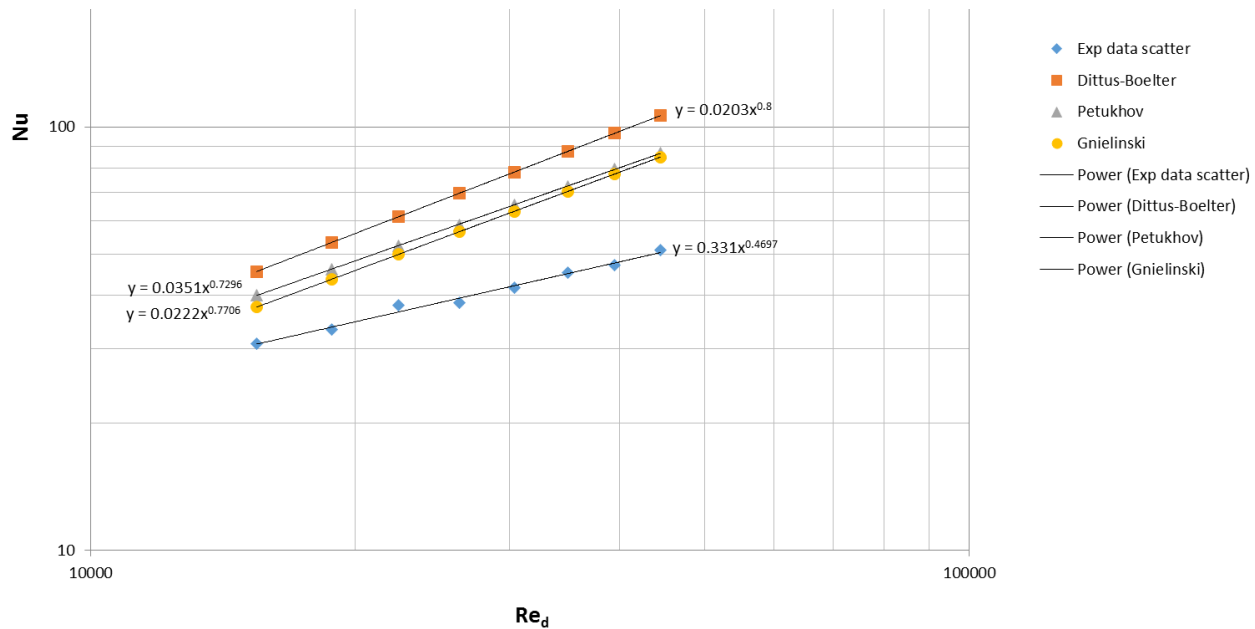


Figure 3. Nu vs Re for 3 channel flow correlations and the experimental data.

As reported below in the attached design report, the expected mass flow rate by computational analysis was 117 g/s. Measured flow rate was 137 g/s at 3600 rpm, maximum blower speed. While this is higher than expected, and higher than ever previously recorded, the agreement with prediction is much closer than other instruments. The flow error would need to be large (factor of 2) to explain the apparent poor cooling performance.

The target was removed and examined to see if there was damage to the part that might explain observations. In particular, a large coolant flow passage toward the rear of the target, away from the instrumented disks, would allow for the high flow rate and yet poor cooling of the instrumented disks. Figure 4 is a photograph of the target after the test. While there appears to be some irregularities in the coolant gaps, the possibility of high bypass flow is not evident.



Figure 4. Photograph of the target, post irradiation and testing.

IR Thermography

The 29 mm window surface temperature was measured using a FLIR A655sc infrared (IR) thermal imaging camera with an 89 mm lens, located 2.5 m from the Inconel window. When measuring surface temperature via IR methods, the resulting measurement is hugely dependent on the surface's emissivity, as well as the transmission through objects such as viewing windows. Without knowing these values, the IR camera is useless in obtaining accurate temperature results. Therefore, the surface emissivity and IR transmission parameters were determined previously using a smaller window in an almost identical fashion at ANL¹. A surface

¹ANL: Argonne National Laboratory

emissivity of 0.422 and a transmission of the entire camera path (reflected off two mirrors and passing through a zinc selenide window), was 0.372. These parameters were input into the FLIR ExaminIR camera software for this experiment in an attempt to achieve accurate temperatures. The camera calibration settings were also adjusted to the appropriate lens size and temperature range. The calibration setting was “FOL89, NOF, 300-2000°C” to account for high surface temperatures.

Figure 5 shows the IR steady state temperature profile at a beam power of 6.42 kW and a helium flow rate of 137 g/s. According to the IR results, the window reached a maximum temperature of 513.4°C. Since thermocouple measurements are not possible on the thin Inconel window, the only method to determine window temperature is by performing simulations. Coupled thermal FEA and CFD simulations were performed by Eric Olivas at LANL to determine a maximum window surface temperature of 107.4°C. The IR result was 406°C greater than the simulation result. This is a significant change. Normally, the emissivity and/or transmission could be adjusted until the IR results matched the expected temperature results (in this case, the simulation results). Unfortunately, the minimum calibration temperature used at the time of the experiment far exceeded the simulated window temperature, so no IR parameter adjustments could be made.

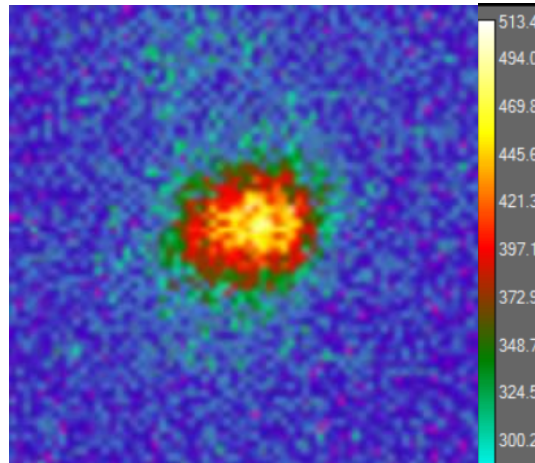


Figure 5. – IR temperature profile of Inconel window ($T_{\max} = 513.4^{\circ}\text{C}$)

Conclusion

The collected data was inconsistent with expectation at the known beam power in every respect. Temperature measurements, both thermocouple and IR, were very high compared with the computational values. Pressure measurements were mutually inconsistent and unreliable. Helium flow rate was higher than expected, but relatively speaking the most

reliable measurement. A lower flow rate or higher beam power would explain the high temperatures observed, but these possibilities were investigated and both highly unlikely.

Meaningful, useful results require a repeat of the experiment. This would need be done with a new target and all instrumentation replaced or confirmed independently.

29 mm Diameter Test Target Design Report

Keith Woloshun, Greg Dale Eric Olivas, Angela Naranjo, Frank Romero

LA-UR-16-27128

8/15/16

Introduction

The Northstar target for Mo99 production is made up of Mo100 disks in a stack separated by coolant gaps for helium flow. A number of targets have been tested at ANL for both production of Mo99 and for thermal-hydraulic performance. These have all been with a 12 mm diameter target, even while the production goals have increased the diameter to now 29 mm. A 29 mm diameter target has been designed that is consistent with the ANL beam capabilities and the capabilities of the helium circulation system currently in use at ANL. This target is designed for 500 μ A at 35 MeV electrons. While the plant design calls for 42 MeV, the chosen design point is more favorable and higher power given the limits of the ANL accelerator. The intended beam spot size is 12 mm FWHM, but the thermal analysis presented herein conservatively assumed a 10 mm FWHM beam, which results in a 44% higher beam current density at beam center.

Design

The new 29 mm target is designed to maintain the same helium flow to maintain the same heat transfer coefficient on the target and window. That target had 25 disks 1 mm thick, with 26 coolant channels 0.5 mm thick, or 126 mm² flow channel total area. This flow area is preserved in a 10 disk target at 29 mm diameter, with 11 coolant gaps. The total disk thickness is limited by the target holder which is mounted to a stalk, the size of which is the basis for the cask design.

The disk thickness varies within the target, as shown in Figure 1, with 5 disks 1 mm thick, 3 at 1.5 mm thick and 2 at 2 mm thick. The target on the stalk is shown in Figure 2, illustrating the limit on target thickness imposed by the target width.

The window design is shown in Figure 3. Made of Inconel 718 as for previous windows, the center thickness is 0.025" (0.635 mm). The pressure side is flat, while the external vacuum side is radiused to increased strength as the beam power diminishes radially.

One additional design change has been introduced. For the previous tests on 12 mm disks, the helium tubing into and out of the target was round tubing until just before and after the target, where a tapered transition to the required rectangular cross-section is required. In the current design, the round to rectangular transition is made at the vacuum boundary entrance, or the brim of the top hat design (Figure 4). The effect of upstream entrance conditions has not been previously investigated.

Figure 5 shows the top hat assembly with the target installed and surrounding shielding. Top hat size is unchanged from the preceding experiments, so the shielding also remains the same.

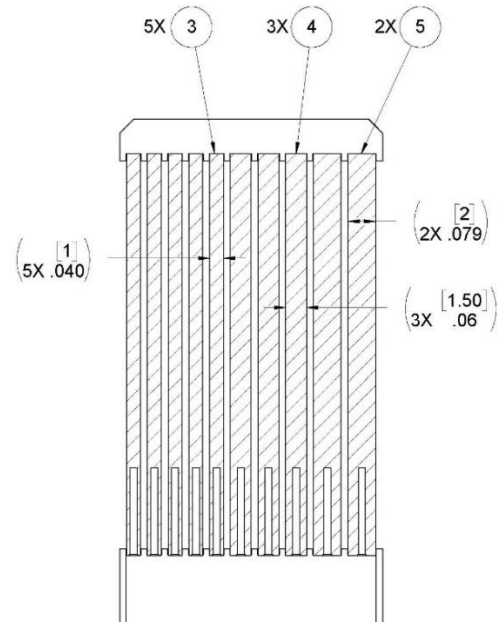


Figure 1. Cross-section view of the target disks in the disk holder. Dick thickness increases with distance from the beam entry window.

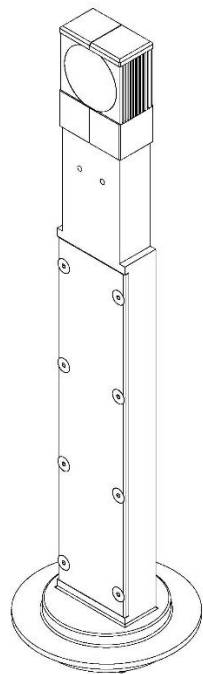


Figure 2. Target as mounted on the stalk. Target is loaded into position from below to facilitate removal by gravity into a cask.

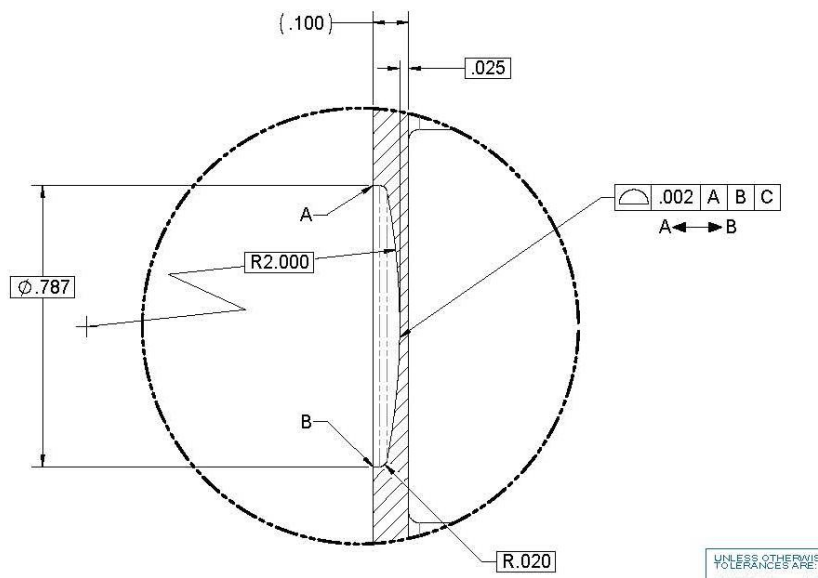


Figure 3. Beam entry window detail.

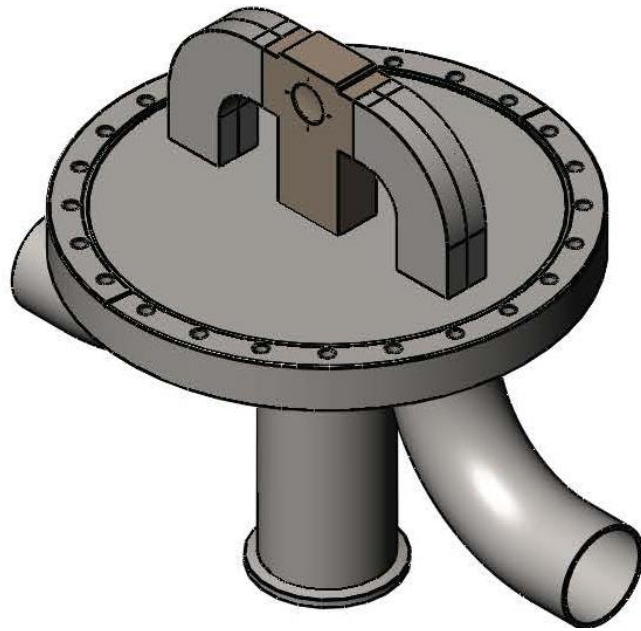


Figure 4. Plumbing configuration into and out of the target. Rectangular entrance and exit geometry matches the channel within the target holder.

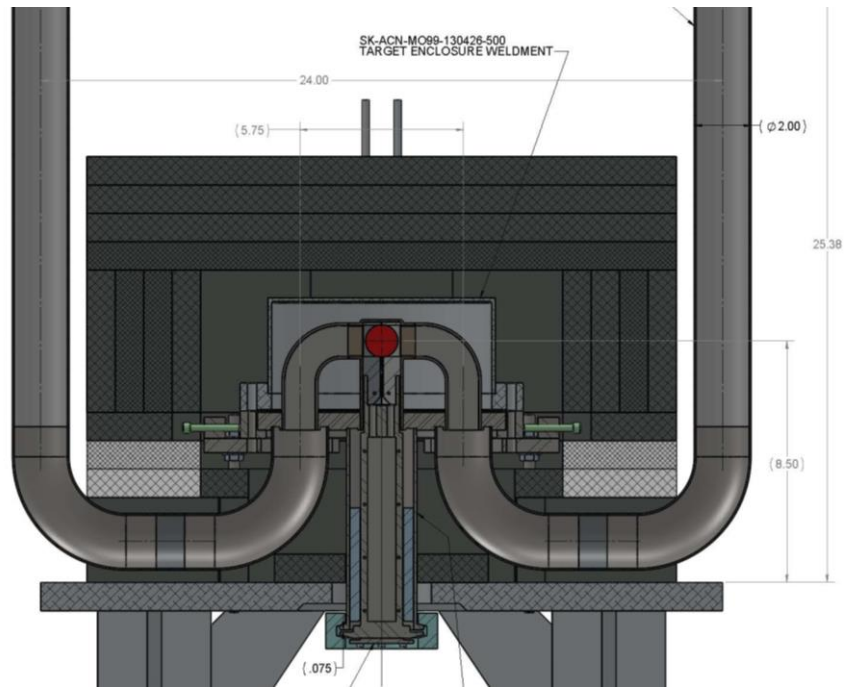


Figure 5. Cross-section view of the overall assembly. The top hat connects to the beam pipe vacuum. Target is illustrated in red. Pb shielding surrounds the top hat enclosure.

Analysis

MCNPX was used to establish the heating in the window and disks at the design current and energy of 500 μ A and 35 MeV. While the intended beam spot size is 12 mm, historically a smaller beam spot is the experimental reality. With that in mind, the analysis was done for a 10 mm FWHM beam, which delivers volumetric heating 44% higher at the peak as compared to 12 mm FWHM. The radial distribution of heat thus established was analyzed using ANSYS conjugate heat transfer code. As blower pressure rise defines our flow limits, inlet and outlet pressure are the boundary conditions on the helium flow in this analysis, 1.965 and 1.8615 MPa (285 and 270 psi), respectively.

Helium velocity in the channels is nominally 242 m/s, shown in Figure 6, with a resulting mass flow rate of 117 g/s. temperature profile through a target center section is shown in Figure 7, and peak temperature in the window and disks is shown in the bar chart (Figure 8).

Stress analysis in the window is a combination of primary pressure induced stress and secondary thermal expansion induced stress. By ASME BPVC, the primary stress must be less than the material UTS/3.5 at the temperature of the location where that stress is indicated. Primary stress only is shown in Figure 9. Peak stress is 255 MPa at the window center where the temperature is highest. UTS at 320 C for annealed 718 Inconel is 828 MPa, based on recent measurements, resulting in allowable stress of 237 MPa. This is slightly below calculated stress, but the difference is small and the analysis was done for a beam spot considerably smaller than the design. Further, ASME code is a very conservative standard for a short-lived experiment.

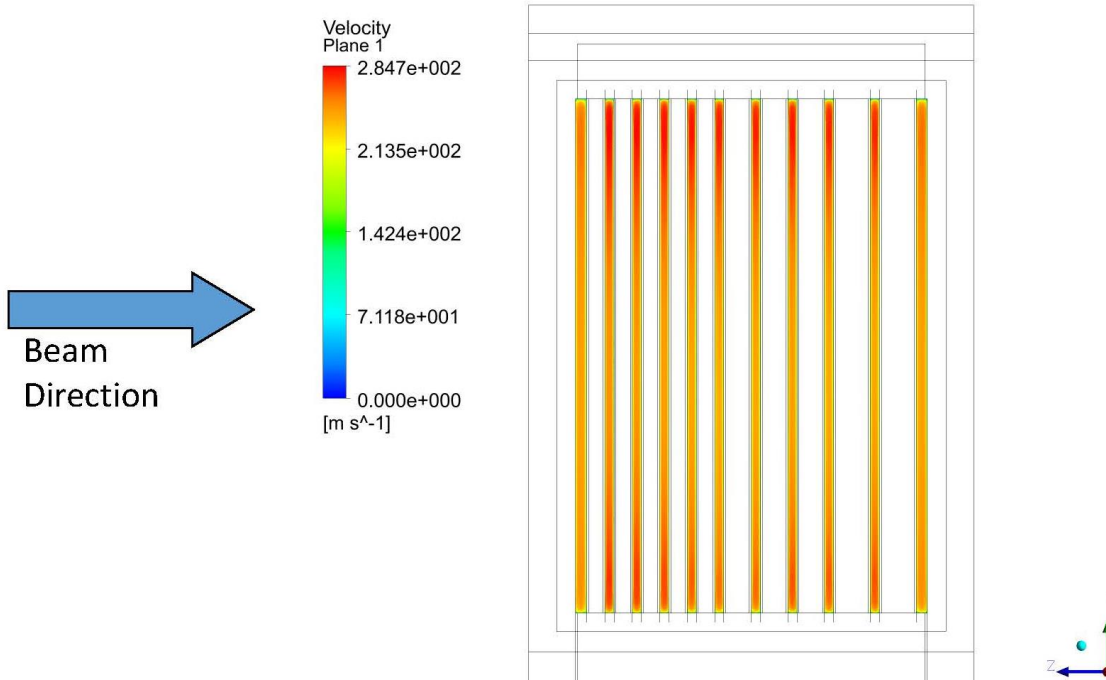


Figure 6. Helium velocity through the channels between disks.

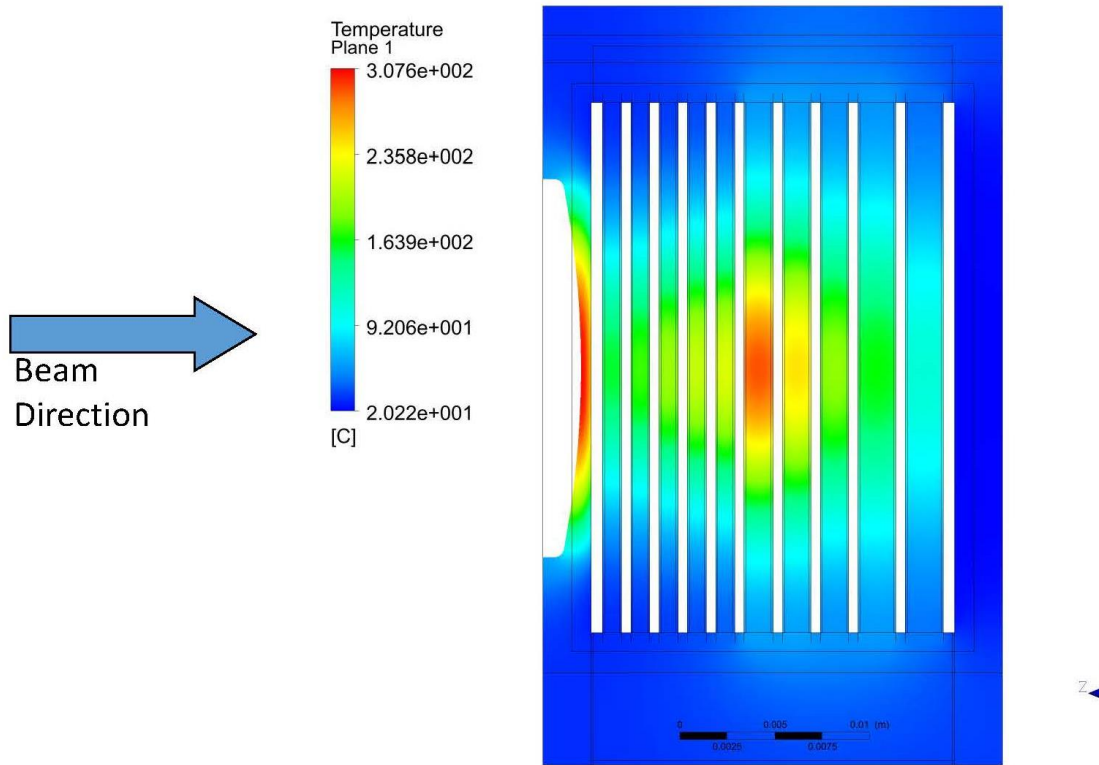


Figure 7. Temperature profiles in the disk and window. Section cut is through the center normal to the helium flow direction.

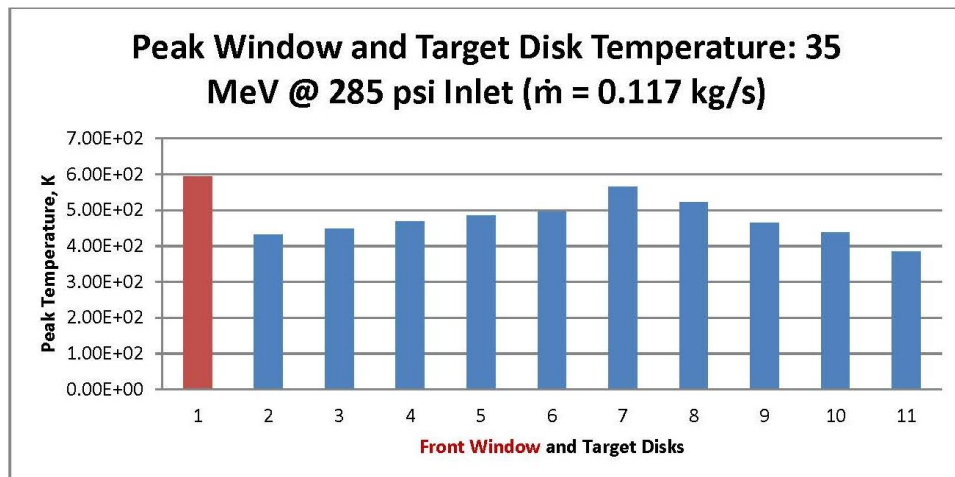


Figure 8. Bar chart illustrating peak temperature in the window and each disk.

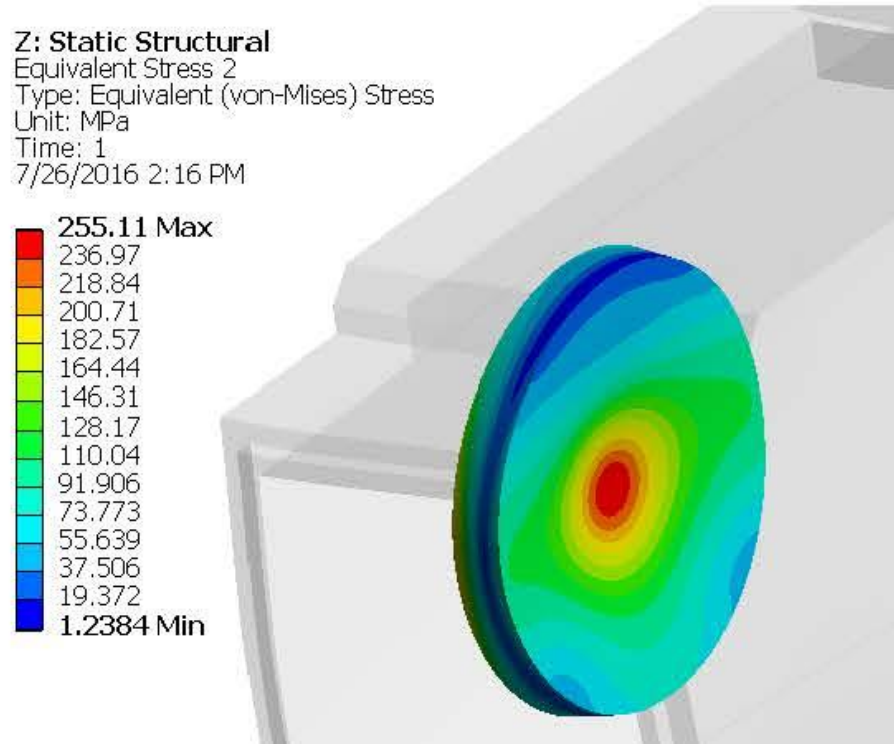


Figure 9. Window primary stress analysis result.

The combined thermal plus pressure induced stress is shown in Figure 10. By code, this combined stress must be less than 3 times the allowable stress, 711 MPa. This is clearly the case. This result indicates that a slightly thicker target, at center, would decrease primary stress while maintaining the thermal and combined stresses within ASME allowables. The current design is considered sufficient, no further iterations on the geometry will be done.

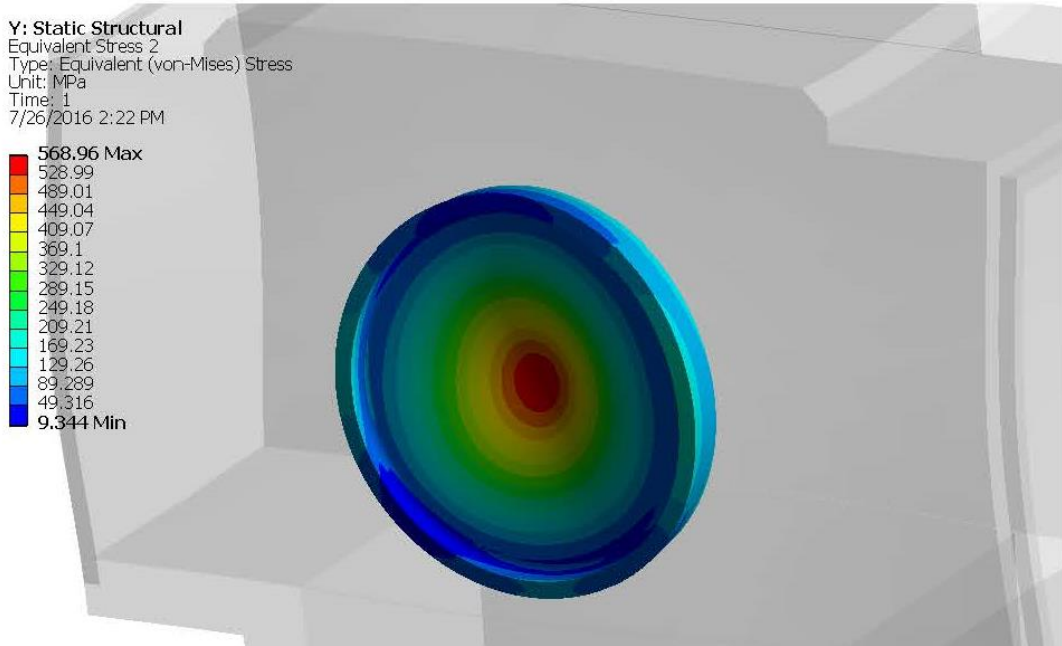


Figure 10. Combined primary and secondary (pressure and thermal) stresses.

Conclusion

A 10-disk, 29 mm diameter target has been designed for testing in the ANL electron beam at 35 MeV and 500 μ A. This will be the first test of a target at this diameter, and also the first test of a target with varying disk thicknesses. A third variation from tests up to now is the rectangular flow channel approach and exit to the rectangular target holder. This is in contrast to an abrupt round to rectangular transition just at the entrance and exit, as has been used previously.